Conference Proceedings

Solar World Congress 2015
Daegu, Korea, 08 – 12 November 2015

SOLAR HOT WATER PRODUCTION BY USING LATENT HEAT STORAGE UNDER TROPICAL CONDITIONS

M.S. Naghavi[1], K.S. Ong[2], I.A. Badruddin[1], H.S.C. Metselaar[1], M. Mehrali[1], A.R. Akhiani[1]

[1] Center for advance materials, Department of Mechanical Engineering, Faculty of Engineering, University of Malaya, Kuala Lumpur (Malaysia)

[2] Department of Industrial Engineering, Faculty of Engineering and Green Technology, Universiti Tunku Abdul Rahman, Kampar (Malaysia)

Abstract

This paper reports a theoretical study about the thermal performance of the new design of solar water heater with a latent heat storage unit. The new design is a solar water heater system consisting of an array of evacuated tube heat pipe solar collectors connected to a common manifold filled with phase change material and acting as a latent heat storage tank. Solar energy incident on the evacuated tube is collected and stored in the latent heat storage tank. The stored heat is then transferred to the domestic hot water supply via a finned pipe placed inside the tank. The performance is analyzed based on an accurate set of mathematical equations. The various climatic conditions of a tropical region are considered as operating environment of the device. The thermal performance of the new design is compared with the conventional evacuated tube heat pipe solar water heater to have a better observation about the differences and advantageous of the new design. The results showed that the thermal performance of the proposed system is higher than a conventional system at certain conditions, which depend to the weather conditions and flowrates, but the sensitivity of the efficiency of the proposed system to the supply water flowrate is less than the conventional system.

Keywords: *solar water heater, evacuated tube, heat pipe, phase change material, thermal energy storage, comparative study*

1. Introduction

Many different combinations of solar thermal systems in integration with phase change material (PCM) for latent heat storage (LHS) have been developed for hot water production, air heating/cooling and power generation [1-6]. Using LHS for solar water heating (SWH) systems received many attractions by researchers. In most of the designs, the PCM was placed in the storage tank [7-13]. A general finding from the most of these researches is that under certain conditions such as system configuration, type of PCM, inlet water temperature and water flow rate, there are improvements in the performance of the SWH-PCM systems.

Al-Hinti et al. [13] experimentally investigated the performance of water-PCM for use with conventional SWH systems. PCM contained in small cylindrical aluminum containers. It was found that the use of the suggested configuration could result in a 13-14^{o}C advantage in the stored hot water temperature over extended periods of time. The hot water storage performance was also investigated when connected to flat plate collectors in a closed-loop system with conventional natural circulation. Over a test period of 24 hour, the stored water temperature remained at least 30^{o}C higher than the ambient temperature. The use of short periods of forced circulation was found to have minimum effect on the performance of the system. Nallusamy and Velraj [14] investigation on a packed bed combined sensible and latent heat storage unit integrated with solar water heating system. It was observed that the mass flow rate has a significant effect on the heat extraction rate from the collector, which in turn affects the rate of charging of the thermal energy storage (TES) tank.

Varol et al. [15] attempted to forecast the performance of a solar collector system using PCM in the hot water storage tank and compared the collector efficiency with the convectional system. In this design, PCM was placed to the bottom of the collector and hot water pipe lines were pathing under the absorber plate, through the PCM slab. It was found that the solar collector system with PCM is more effective than convectional systems. Padovan and Manzan [16] developed an algorithm to optimize a simple configuration of the SWH, which features a plane solar collector, a boiler and a PCM enhanced tank. In parallel with the optimization a sensitivity analysis was carried on in order to find out the relation between the design parameters of the tank

doi:10.18086/swc.2015.02.11 Available at http://proceedings.ises.org

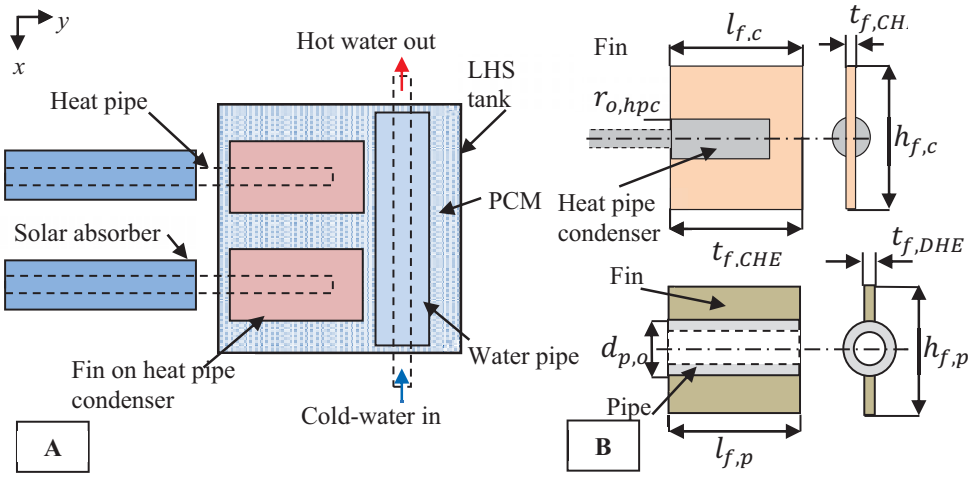

Fig. 1: A. HPSC-PCM system; B. Fin designs for condenser shell (top) and water supply pipe (bottom)

(geometry, phase change temperature of the PCM, and insulation) and the performance of the system. The main outcome of this research was that for this design, the PCM did not have major impact on the results, while other parameters play a more significant role.

To the authors' knowledge, although there are few research works on the combination of heat pipe solar collectors and PCMs in storage tanks [17, 18], there is no work done on the proposed HPSC-PCM system where there is an intermediate heat exchanger on the manifold (condenser side) of the heat pipe. A new HPSC-PCM system is described in the following section. This research plans to examine, analytically, the feasibility of this system in different climatic conditions in a tropical country (Malaysia). The charging/discharging processes during the day/night times are determined. The performance of a conventional HPSC (HPSC-C) theoretically compared with this innovative design. PCM melting/solidifying processes are determined by a one-phase Stefan problem quasi-stationary approximation method, which is one of the more widely used standard analytical solutions. Calculations are done by a computational code developed in Matlab.

2. A description of the proposed system

Fig. 1A displays the recommended HPSC-PCM system which comprises an arrangement of evacuated tube heat pipe solar collectors linked to a shared manifold loaded with PCM. This manifold functions as a LHS tank. The evaporator segments of the heat pipes are subjected to solar radiation while the condenser segments are slotted into finned sockets which have been inserted onto the manifold. The evaporator performs as an absorber of solar energy which is then conveyed to the condenser by way of heat pipe action involving evaporation and condensation. This energy is stockpiled in the PCM-filled LHS tank. Household cold water delivered by way of a finned pipe rises in temperature as it makes its way through the LHS tank. Heat transfer efficiency is raised through the welding of single-row vertical fins onto the heat pipe condenser shell and also onto the finned pipe line (Fig. 1B). Table 1 exhibits the dimensions of the LHS tank, HPSC and fins.

3. Hypothetical model

This section provides a concise presentation of equations for the arithmetical modelling of heat transfer. A comprehensive array of equations and flow charts was forwarded in a previous paper [19]. During the process of charging and discharging of heat within the PCM, three separate heat transfer developments take place. To begin with, the evaporator section of the HPSC soaks up heat from solar energy which is then conveyed to the condenser section. Subsequently, the heat transfers to the PCM through the condenser shell. The accumulated heat discharges from the PCM to the finned pipeline and warm up the water passing through it. The computations for these procedures are carried out separately and in accordance to the sequence during which they take place.

3.1. Charging mode

The main factors influencing absorbable solar radiation are ground reflectance, angle and the material employed as collector. For the purpose of assessing these factors, we harnessed the process launched by Duffie and Beckman [20]. The temperature of heat pipe segments was ascertained through an equation forwarded by Zue and Vafai [21]. Through this equation, a methodical resolution to problems related to the surface temperature along the span of a low temperature heat pipe can be realized.

Table 1, Dimensions of LHS tank, HPSC and fins

Manifold and Evacuated tube		Heat pipe	
Item	Value	Item	Value
Number of heat pipes	20	Evaporator length (mm)	1675.00
Glass tube outer diameter (mm)	58	Adiabatic length (mm)	30.00
Glass tube thickness (mm)	2	Condenser length (mm)	70.00
Absorber plate thickness (mm)	1	Evaporator outer radius (mm)	4.00
Evacuated tube length (mm)	1675	Condenser outer radius (mm)	12.00
Fin thickness on the CHE (mm)	2	Wall thickness (mm)	0.50
Storage tank height (mm)	204	Wick thickness (mm)	1.00
Storage tank width (mm)	204	Vapor core radius (mm)	3.00
Storage tank length (mm)	1725	Thermal conductivity of liquid (W/mK)	0.63
Fin height on the CHE (mm)	200	Thermal conductivity of wall (W/mK)	385
Fin length on the CHE (mm)	200	Porosity	0.5
Fin thickness on DHE (mm)	2	Permeability	1.5×10^{-9}
Fin height on DHE (mm)	91	Thickness of the fiber (mm)	2×10^{-7}
Pipe outer diameter (mm)	18	Number of meshes per unit length	4000
Length of a section (mm)	142		
Slope of solar collector (°)	20		
Glass emittance	0.88		
Plate emittance	0.95		
Reflective Index of glass	1.53		

The PCM heat equation is deemed a 2nd order linear partial differential equation with heterogeneous boundary conditions. As the transfer of heat from the condenser shell to the PCM occurs in an arrangement that is similar for both sides, computations for the PCM are ascertained based solely on one side of the condenser shell. A significant presumption regarding the quasi-stationary one-phase Stefan problem is that the hot plate (which is the finned condenser shell) is subjected to a consistent temperature. Also presumed is that heat transference from the fin on the shell to the PCM is a one-dimensional occurrence and that the temperature of the PCM at the outset is at melting point.

Expressed as $T(x,t)$, the PCM temperature is a function of position and time. At a consistent temperature, a slab of the PCM ($0 \le x \le l$) is deemed to be solid. The imposed temperature at the interface of the PCM and the HPC fin facilitates the transference of heat through the PCM. It is taken for granted that the remaining three edges are in an insulated state. The following is an expression of the mathematical model for the one-dimensional transient heating procedure.

$$\rho_s c_s \frac{\partial T}{\partial t} = k_s \frac{\partial^2 T}{\partial x^2}, \qquad \text{(eq. 1)}$$

It is essential that this equation be solved in accordance to the preliminary and boundary conditions for the scale of $0 < x < X(t)$:

$$T_{pcm}(0,t) = T_{hp}(t), \qquad \text{(eq. 2a)}$$

$$T_{pcm}\big(X_{pcm}(t),t\big) = T_m, \qquad \text{(eq. 2b)}$$

$$\rho_l L {X_{pcm}}'(t) = -k_l \frac{\partial T_{pcm}}{\partial t}|_{x=X_{pcm}(t)}, \qquad \text{(eq. 2c)}$$

$$X_{pcm}(0) = 0 \qquad \text{(eq. 2d)}$$

where X(t) denotes the position of the interface. The heat equation is rendered exceedingly complex by the need to meet boundary conditions (eq. 2c). In line with the Neumann solution to the one-phase Stefan problem [22], the quasi-stationary solution for expressing the interface position and temperature dissemination in the PCM (in the context of primary physical variables related to the charging procedure) assumes the following configuration:

$$X_{pcm}(t) = \eta_{f,c}\sqrt{(2k_l St_l t)/(\rho c_l)} \qquad \text{(eq. 3)}$$

$$T_{pcm}(x,t) = T_{hpc}(t) - \Delta T_l \frac{x}{X_{pcm}(t)}, 0 \le x \le X_{pcm}(t), \qquad \text{(eq. 4)}$$

where, $\Delta T_l = T_{hpc}(t) - T_m$.

The heat transfer from the object to the surrounding material is accelerated by the presence of fins on the condenser shell. Consistency in terms of heat dispersal on the surface of the fin was taken as fact. For the purpose of incorporating the impact of this presupposition into the computation procedure, the effectiveness of the fin is roped in through the array of equations cited in [19].

3.2. Discharging mode

As portrayed in Figure 2, the PCM within the LHS tank is split into a fixed number of slabs (*j*). Each slab is subjected to the application of energy balance. The outlet water temperature of each slab matches that of the inlet water temperature of the neighbouring slab. The inlet water temperature determines the pace of PCM solidification for every slab. The finned pipe is positioned at the centre of the tank. This serves to partition every slab into two identical segments on both the upper and lower sides of the finned pipe. Both sides of the fin come into play during the heat transfer process.

The solidification of the PCM is attributed to the flow of cold water into the storage tank at a velocity of *v* and a temperature of $T_{w,i,i}$. Each slab's solid-liquid interface progression speed and their outlet water temperature are the undetermined variables. It is essential that the verification of these variables be carried out in unison. It is supposed that in the event the Stefan number is inconsequential ($St < 2$) during the discharging procedure, the temperature of the PCM will stay unremittingly within reach of melting point while the solid-liquid interface is advancing [22]. Hence, the supply water temperature rises in tandem with the solidification process of the slab *j*. Subsequent to complete solidification, slab *j* loses its thermal inertia, its temperature will quickly decline to match the inlet water temperature at its location, and the water will swiftly react to one fewer slab. In other words, at the outset, *N* slabs were raising the temperature of the supply water. However, upon the solidification of the initial PCM slabs, the supply water temperature elevation was attributed to *N-1* slabs. The presumptions that require contemplation for the application of this solution process are: (a) during the process of discharging, the transference of thermal energy from the PCM to the finned pipe is exclusively one-directional (i.e. on the *y* axis), (b) when the fall in the axial temperature is not excessive, the transmission of heat in the direction of x can be disregarded, (c) heat conduction within water that is thermally stable is inconsequential, (d) the latent heat of the PCM is so substantial that the surface temperature of the PCM at the fins and walls of the pipe can, for the most part, be deemed equivalent to T_m during the whole process of solidification. This presumption is believable if one takes into consideration the fact that with a raised latent temperature (insignificant Stefan number), the front will not make much headway into the PCM, while an elevated degree of conductivity will lead to the tendency to round up the temperature. In a situation where the PCM does not melt completely during charging, it follows that during the discharging process only the PCM molten mass fraction is regarded as an active mass of the PCM slab.

Heat transference to the finned pipe from the melted PCM is realized through:

$$\dot{q}(t) = \dot{q}_p(\mathrm{t}) + \dot{q}_{f,p}(\mathrm{t}) \qquad \text{(eq. 5)}$$

where $\dot{q}_p(\mathrm{t})$ denotes the heat flux to the pipe and $\dot{q}_{f,p}(\mathrm{t})$ denotes the heat flux through the fins. An array of equations for ascertaining the heat flux can be observed in [19].

Efforts to determine the solidification time of the PCM slabs necessitate a repeat solution to eq. 1 with altered initial and boundary circumstances. In such a situation, it is imperative that the heat equation be worked out in accordance with the imposed heat flux ($\dot{q} < 0$):

$$T_{pcm}(x,0) = T_m, \qquad \text{(eq. 6a)}$$

$$\rho_s \bar{L} Y_{pcm}{}'(t) = -k_s \frac{\partial T_{pcm}}{\partial t}\Big|_{y=Y_{pcm}(t)}, \qquad \text{(eq. 6b)}$$

$$-k_s \frac{\partial T_{pcm}}{\partial t}\Big|_{y=0} = \dot{q}(t), \qquad \text{(eq. 6c)}$$

$$Y_{pcm}(0) = 0 \qquad \text{(eq. 6d)}$$

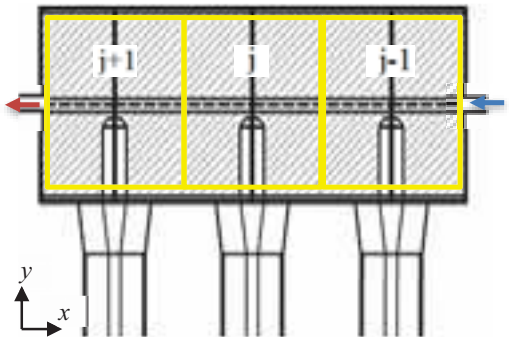

Fig. 2: Arrangement of PCM slabs

In this approach, a molten slab at its melt temperature of T_m is undergoing solidification through an imposed flux $\dot{q}(t)$ at the exteriors of the fins. In line with the Neumann solution technique for the management of a one-phase quasi-stationary Stefan problem, the inclusion of initial and boundary conditions gives rise to the following equation for the solid-liquid interface location:

$$Y_{pcm}(t) = \dot{q}(t)\, t/\rho_s\, \bar{L} \qquad \text{(eq. 7)}$$

In a circumstance where the temperature of the molten PCM slabs exceeds that of the melting point, the effect of stored sensible heat can be realized by modifying the latent heat magnitude through the following equation [22]:

$$\bar{L} = L + \frac{1}{2} c_l (T_L - T_m) \qquad \text{(eq. 8)}$$

where $T_L = mean\left(T_{pcm}(x = 0{:}\, l_{pcm}\,, t_{end})\right)$ represents the mean temperature of the PCM at the culmination of the melting time.

3.3. Exploitable heated water and performance efficiency

In this segment, an evaluation is conducted on the effectiveness of the recommended scheme in comparison to a conventional scheme. In a conventional scheme (deemed a baseline system), heated water is amassed in a tank without any draining off of water in day time. The effectiveness and potential of a scheme for hot water delivery can be determined through a calculation involving the effects of stratification.

The baseline SWH system entails the passage of cold water directly across the heat pipe condenser in the manifold. The resulting hot water is then amassed in an insulated reservoir. The degree of heat transfer from the condenser to the supply water can be ascertained through equations which are also used for computing the temperature of the heat pipe surface (refer to Section 3.1). The equations for calculating heat transfer from the condenser to the supply water can be observed in [19].

Solar heat is accumulated during daylight hours and saved in the storage tank. No water is drawn out during daytime. The main purpose of the storage tank is to preserve the temperature of the heated water. It is thus essential that the degree to which heat diminishes over time be calculated. Natural thermal stratification is a significant factor in operations involving the storage of heated water in a tank[23]. Even in a circumstance where there is no water draw-off, heat convection from the hot water layer to layers of a lower temperature, and vertical conduction in the wall of the storage tank can lead to destratification [24].

Of late, a study conducted by Armstrong et al. [25], succeeded in establishing the destratification-related deficit rate of utilizable heated water in a reserve tank. This investigation revealed that a 74 litre capacity copper tank with a thickness of 0.7mm, and cladded with an outer 50mm layer of rigid polyurethane insulating foam (0.028 W/mK) [26], underwent a usable hot water volume loss rate of 2.1 litres per hour over a period of 12 hours. A division of the tank capacity by the usable volume loss rate led to the presumption that 3% of usable heated water in the tank will be done away with. An additional presumption is that the loss of heat to the environment from the wall of the tank is insignificant in comparison to the conjugate exchange with the water.

In the opinion of Armstrong [23] the utilizable heated water volume is identical to the volume of fluid from a tank that can be mixed to a favourable ultimate operational temperature (T_u.) The utilizable heated water volume can be calculated through the equation:

$$V_u(t) = m_w \times \sum_{hr=1}^{12} \frac{T_{w,t,o}(t) - T_u}{T_u - T_{w,t,i}(t)} \qquad \text{(eq. 9)}$$

Bearing in mind that the tank is deemed to be in an inactive mode, and taking into consideration the usable volume loss rate percentage (*Lr*), the usable volume obliteration can be calculated through the equation below:

$$V_{u,\mathrm{d}}(t) = V_u(t) \times Lr \times (12 - t) \qquad \text{(eq. 10)}$$

The expression $(12 - t)$ denotes the period that the generated heated water in the solar collector will be standing by in the tank. Thus, the volume of left over utilizable hot water after a period of 12 hours can be calculated through the equation:

$$V_{u,\mathrm{r}} = \sum_{hr=1}^{12} V_u(t) - V_{u,\mathrm{d}}(t) \qquad \text{(eq. 11)}$$

As destratification does not transpire in the PCM tank, the presence of detrimental energy in this tank can be discounted ($V_{u,\mathrm{d}}(t) = 0$). In keeping with equations (9) and (11), the volume of usable hot water and total usable hot water generated by the PCM tank is calculable.

The total energy liberated by usable hot water from the water and PCM tanks can be determined through the equation:

The total delivered energy by usable hot water from the water tank and from the PCM tank can be calculated by:

$$E_d = V_{u,\mathrm{r}}\, c_{p,w}\, (T_u - T_{w,t,i}(t)) \qquad \text{(eq. 12)}$$

The systems' energy efficiency is computed through:

$$\eta_{tot} = \frac{E_d}{S} \qquad \text{(eq. 13)}$$

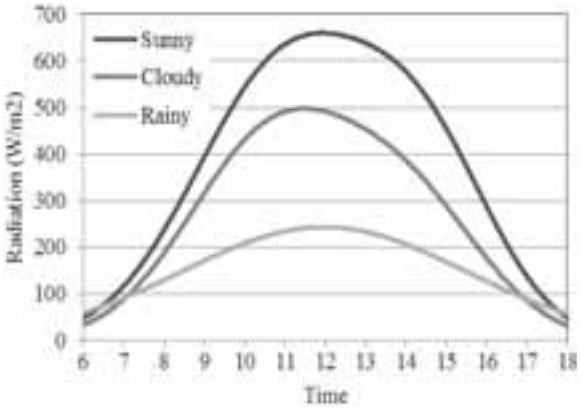

Fig. 3: Solar radiation

4. Results and discussion

The predominant objective of this endeavour is to hypothetically assess the thermal capacity of the combined HPSC-LHS systems for storage in various climate conditions and compare it with the baseline system. In this investigation, water does not flow across the manifold during the day. It is only after sunset, when the system controller allows water to flow through the inbuilt pipe in the tank, then the system is in discharging mode. The precision of this hypothetical approach is examined in [19].

Authentic meteorological data stretching over a time span of two years (2008-2009) was acquired from the Kuala Lumpur International Airport meteorological station (Lat. 2.44°& Long. 101.42°) to assess the twelve-monthly solar radiation concentration. As for the daily solar radiation, the days were classified as sunny (I>18 MJ/m^2/day), cloudy (18>I>13 MJ/m^2/day) and rainy (13>I MJ/m^2/day) days. The average solar radiation level for each classification is displayed in Figure 3.

4.1. PCM charging and discharging processes

At the outset, the PCM is in a solid form. The liquefaction process of the PCM is triggered upon its arrival at the melting temperature. Table 2 displays the features of the paraffin utilized as the PCM and copper fin properties. The temperature of the melted fraction climbs unremittingly on condition that the supply of heat is uninterrupted. The rise and fall of the temperature gradient is directly linked to heat flux discrepancies. The efficiency of the finned shell on the heat pipe condenser is approximately 90% for copper materials. As previously stated, the system involves the employment of 20 steel pipes. During charging mode, the storage tank remains on standby and no supply water flows through the pipe. As such, for all 20 slabs, the PCM thermoclines and interface growth designs are identical. Figure 4 portrays the progressions of the liquid-solid interfaces for the three distinct weather conditions. At the conclusion of a sunny day, it was observed that melting of roughly 60mm of the PCM thickness had occurred at each side of the finned shell. As for a cloudy and rainy day, the level of melting was approximately 52mm and 43mm, respectively. It is apparent that during the morning hours, the interface progression rate is accelerated. The two explanations for this circumstance are (a) the elevated temperature gradient between the condenser and the PCM during the morning heating up period and (b) the attendance of liquid PCM surrounding the fin with its intrinsic depleted convective heat transfer coefficient. As heat transmission through the heat pipe takes place purely in one direction, specifically from the evaporator section to the condenser section (resembling a one-way valve [27]), energy wastage from the storage tank is averted.

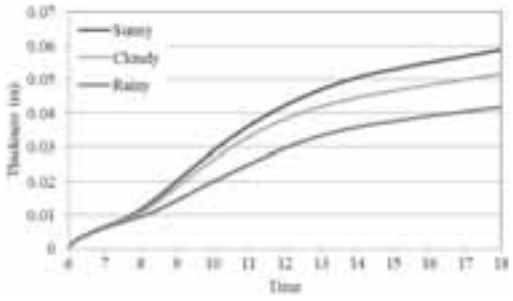

Fig. 4: Liquid-solid interface in charging mode

Tab. 2: Physical properties of paraffin wax and copper fins [28, 29]

Property	PCM	Fin (Solid)
Melting point (°C)	64	-
Density solid / liquid at 15/70°C (kg/m^3)	990 / 916	2713
Thermal conductivity of solid / liquid (W/mK)	0.349 / 0.167	380
Specific heat solid / liquid (kJ/kgK)	2.76 / 2.48	0.96
Volume expansion at ΔT=20°C (%)	0.293	-
Heat storage capacity (kJ/kg)	174	-
Dynamic viscosity (kg/ms)	0.00385	-

While the heat transfer route in the charging mode runs parallel to the *x* axis, in the discharging mode it runs parallel to the *y* axis (Figure 1). It is taken for granted that the discharge procedure begins subsequent to sunset as soon as the controller permits the flow of supply water through the finned pipe. Due to the fact that in the discharging mode, the transference of convective heat within the pipe is paired to heat deletion from the PCM, the most significant parameters to scrutinize in the storage reservoir are the outlet water temperature and solid-liquid interface progression of the various slabs.

As described in Section 3.2 and Figure 2, as a result of the elevation in water temperature while flowing through the finned pipe during discharging mode, the phase alteration performance of the PCM fluctuates across the span of the storage tank. In both rectangular slabs, heat transfer from the molten PCM to the finned pipe is symmetrical. The progression of the solid-liquid interface in relation to three slabs of the PCM tank for two flow rates and three weather conditions is exhibited in Figure 5. The outcomes imply that former PCM slabs experience solidification quicker than latter ones. This is attributed to the greater temperature disparity of the inlet supply water and PCM.

Owing to the elevated temperature of the molten PCM at the extremity of the charging mode (refer to Equation 8), a customized latent heat value of 229*kJ/kg* was utilized to ascertain the interface progression.

4.2. Temperature of supply water

The simulation outcomes for the outlet supply water temperature after 18:00 at flow velocities of 50 litres and 70 litres per hour (lph) are displayed in Figure 6. The inlet cold water temperature is maintained at 29ºC. An elevation in the flow rate brings about a decrease in the system's operating time. The proposed operational temperature for household usage is between 38ºC and 41ºC [30]. For this study, the operational temperature was presumed to be 40ºC. As such, the system's operating time with an outlet water temperature in excess of 40ºC is downgraded from more than four hours to just about three hours. The maximum outlet supply water temperature on days that are sunny was recorded as 53ºC for a flow rate of 50 lph, and close to 47ºC for a flow rate of 70 lph.

The HPSC-C system equipped with 20 heat pipes was simulated at two flow rates for three weather conditions to evaluate the outlet water temperature. According to the graphs, the peak usage period is during noontime, and the highest hot water temperatures in the HPSC-C system in various circumstances are below

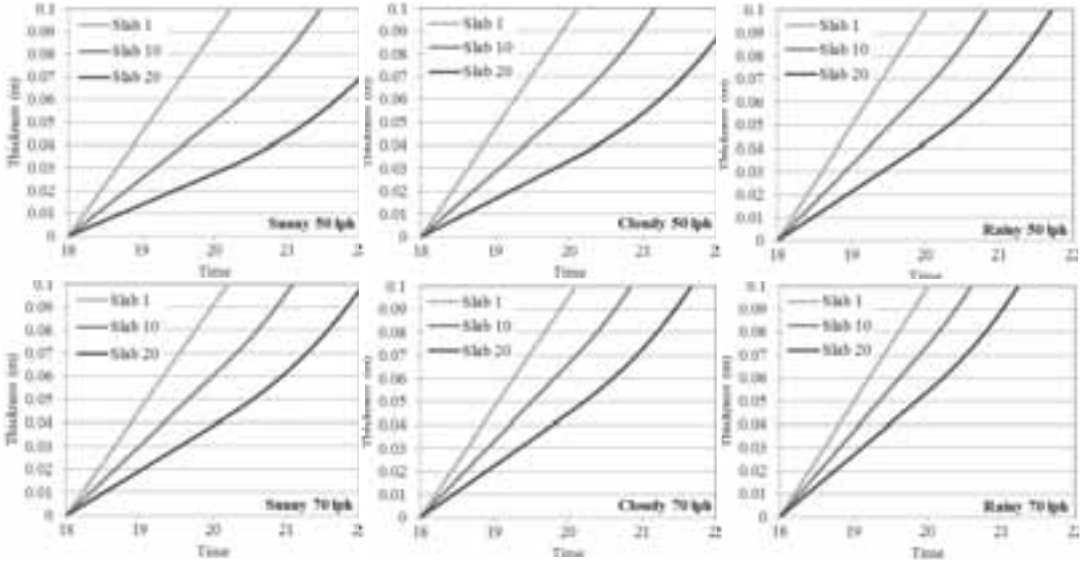

Fig. 5: Progression of solid-liquid interface in slabs 1, 10 and 20 of PCM tank

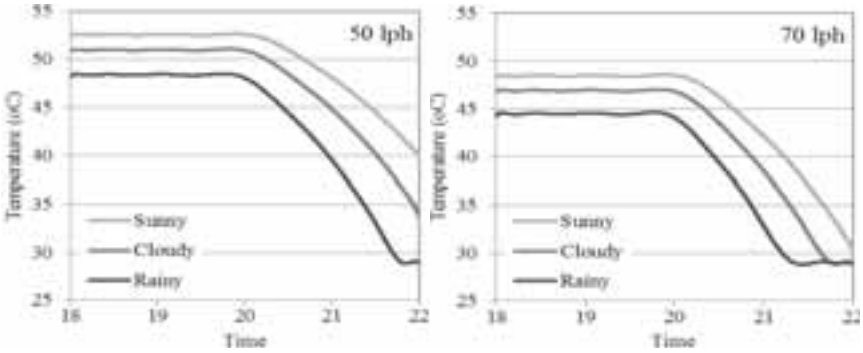

Fig. 6: Outlet supply water temperature ($T_{w,i,o}$) for ETHPSC-PCM system

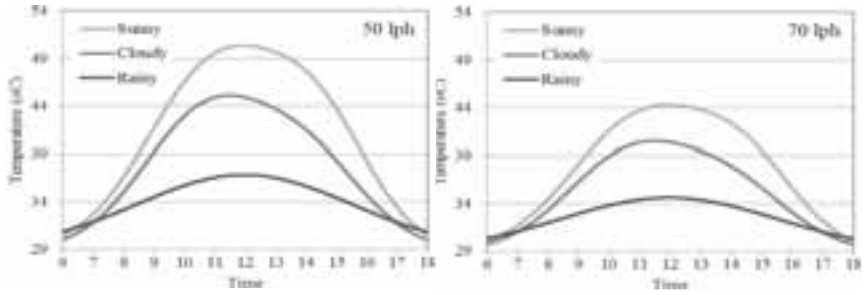

Fig. 7: Outlet water temperature ($T_{w,b,o}$) for ETHPSC-C system

those in the HPSC-PCM system. As the demand for domestic heated water is at its highest at sundown, the usefulness of the recommended system is enhanced by the moving of the peak time to this period.

4.3. Comparative investigation

In order to compare the baseline and proposed systems, it is presumed that the produced hot water in the storage tank of the baseline system remains in the storage tank until evening. The releasing water from the hot water storage tank and the LHS tank start at the same time. As the temperature of the outlet water from the tank is above that of the operating temperature (39°C), it is essential that it be mixed with cold water (29°C).

The scale of generated heated water at operating temperature as well as the total effectiveness of the systems can be approximated through the equations presented in Section 3.3. A comparison between the HPSC-PCM system and the HPSC-C system in terms of efficiency (η_{tot}) and usable volume (V_u) for two flow rates and

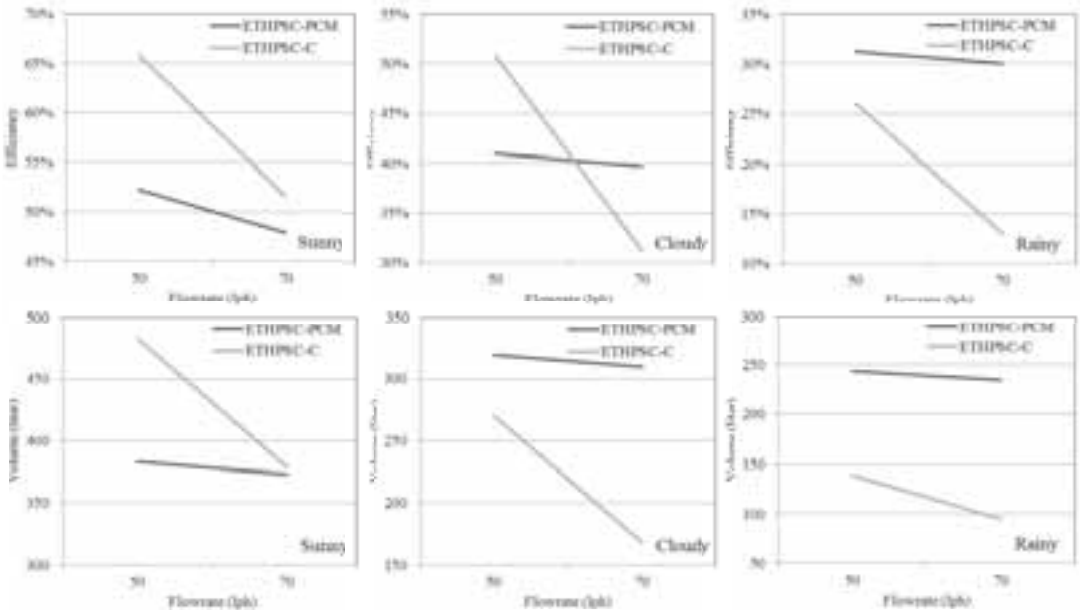

Fig. 8: Comparison of efficiency and usable hot water volume

three weather conditions are shown in Figure 8. As the thermal operational level of the HPSC-C system plunges drastically upon elevations in the draw-off flow rates, it follows that the volume of usable heated water also plummets. As for the proposed system, by increasing the flowrate, although a decrease in thermal efficiency is unavoidable, this decrease is not as rapid as in the conventional system. On a sunny day, the efficiency of the HPSC-PCM system ranges between 53% and 48% upon an elevation in the flow rate from 50 lph to 70 lph. Under a similar circumstance, the efficiency level of the HPSC-C fluctuates between 61% and 52%. During harsh (rainy) weather conditions, the effectiveness of the HPSC-C system ranges from 26% at 50 lph, to below 13% at 70 lph. In a similar situation, the efficiency of the HPSC-PCM system varies between 32% and 30%. Generally, the efficiency range of the HPSC-PCM system extends between 53% and 30%, while that of the HPSC-C system stretches between 65% and higher to 14% and below. This is an indication that the innovative system is superior to the conventional system in terms of stability. A similar efficiency trend was observed in the context of water capacity. The most outstanding revelation is the fact that the innovative system is capable of offering at least 200 litres of heated water under the harshest of weather conditions, while the conventional system is unable to meet the demand for domestic hot water on rainy, and perhaps even on cloudy days.

To be able to have a more detailed view about the effectiveness of the performance of the HPSC-PCM in a tropical climate, the available data of three meteorological stations in Malaysia for two years were studied. The number of days in a year with different weather conditions are shown in Table 3 and Figure 9. It is observed that averagly 45% of the days in a year are mostly sunny and rests are in mostly cloudy or rainy conditions. According to Figure 9, the ratio of sunny days could be even as low as ~32% in a year. Refer to the Figure 8, both designs have suffiecent performance in sunny days. However, in non-sunny days the new design provide more hot water volume and more stable operation, which this illustrates the advantageous of the new design in comparison with the conventional model.

Tab. 3: Number of the sunny, cloudy and rainy days in a year

Station	Location (Lat./Long.)	Sunny	Cloudy	Rainy
Mersing (2007)	2° 27' N / 103° 50' E	164	121	80
Mersing (2008)	2° 27' N / 103° 50' E	145	136	84
Subang (2008)	3° 07' N / 101° 33' E	188	121	56
Subang (2009)	3° 07' N / 101° 33' E	202	116	47
KLIA (2008)	2° 44' N / 101° 42' E	121	165	79
KLIA (2009)	2° 44' N / 101° 42' E	169	129	67
	Average	**45%**	**36%**	**19%**

5. Conclusion

A hypothetical study was conducted on the feasibility of integrating an evacuated tube heat pipe solar collector and a latent heat storage tank. This study was based on authentic meteorological data as regards to

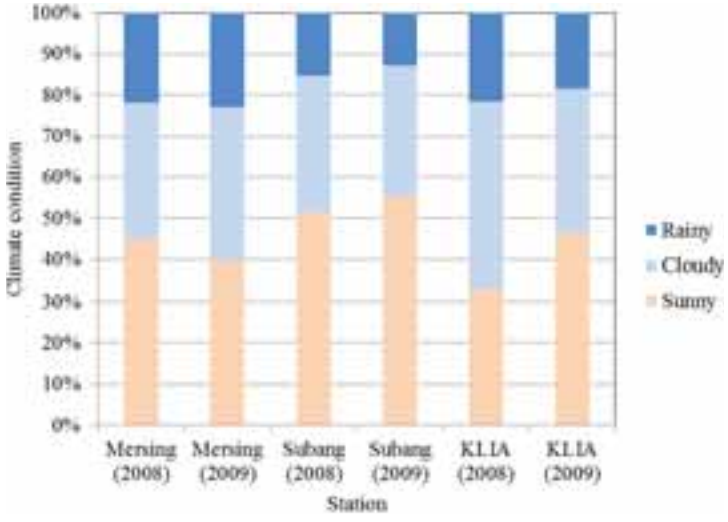

Fig. 9: The ratio of climatic condition during a year

three Malaysian weather conditions. An examination of the HPSC-PCM charging/discharging procedures revealed that under certain circumstances, the thermal performance of the recommended system is superior to that of a standard system. While the HPSC-C system and the HPSC-PCM function are in satisfactory level on sunny days, at a certain flow rate on cloudy and rainy days the HPSC-PCM system exhibited a higher level of effectiveness. This investigation also uncovered that the degree of sensitivity to the supply water flow rate is lower for the recommended system than the conventional system.

6. References

[1] S. Wu, G. Fang, Dynamic performances of solar heat storage system with packed bed using myristic acid as phase change material, Energy and Buildings, 43 (2011) 1091-1096.
[2] H. Benli, A. Durmuş, Performance analysis of a latent heat storage system with phase change material for new designed solar collectors in greenhouse heating, Solar Energy, 83 (2009) 2109-2119.
[3] W. Saman, F. Bruno, E. Halawa, Thermal performance of PCM thermal storage unit for a roof integrated solar heating system, Solar Energy, 78 (2005) 341-349.
[4] G. Serale, F. Goia, M. Perino, Numerical model and simulation of a solar thermal collector with slurry Phase Change Material (PCM) as the heat transfer fluid, Solar Energy, 134 (2016) 429-444.
[5] Z. Liao, A. Faghri, Thermal analysis of a heat pipe solar central receiver for concentrated solar power tower, Applied Thermal Engineering, 102 (2016) 952-960.
[6] S. Esakkimuthu, A.H. Hassabou, C. Palaniappan, M. Spinnler, J. Blumenberg, R. Velraj, Experimental investigation on phase change material based thermal storage system for solar air heating applications, Solar Energy, 88 (2013) 144-153.
[7] N. Nallusamy, S. Sampath, R. Velraj, Experimental investigation on a combined sensible and latent heat storage system integrated with constant/varying (solar) heat sources, Renewable Energy, 32 (2007) 1206-1227.
[8] A.J.N. Khalifa, K.H. Suffer, M.S. Mahmoud, A storage domestic solar hot water system with a back layer of phase change material, Experimental Thermal and Fluid Science, 44 (2013) 174-181.
[9] M. Ibáñez, L.F. Cabeza, C. Solé, J. Roca, M. Nogués, Modelization of a water tank including a PCM module, Applied Thermal Engineering, 26 (2006) 1328-1333.
[10] T. Kousksou, P. Bruel, G. Cherreau, V. Leoussoff, T. El Rhafiki, PCM storage for solar DHW: From an unfulfilled promise to a real benefit, Solar Energy, 85 (2011) 2033-2040.
[11] M. Esen, A. Durmuş, A. Durmuş, Geometric design of solar-aided latent heat store depending on various parameters and phase change materials, Solar Energy, 62 (1998) 19-28.
[12] S. Canbazoğlu, A. Şahinaslan, A. Ekmekyapar, Ý.G. Aksoy, F. Akarsu, Enhancement of solar thermal energy storage performance using sodium thiosulfate pentahydrate of a conventional solar water-heating system, Energy and Buildings, 37 (2005) 235-242.
[13] I. Al-Hinti, A. Al-Ghandoor, A. Maaly, I. Abu Naqeera, Z. Al-Khateeb, O. Al-Sheikh, Experimental investigation on the use of water-phase change material storage in conventional solar water heating systems, Energy Conversion and Management, 51 (2010) 1735-1740.
[14] N. Nallusamy, R. Velraj, Numerical and experimental investigation on a combined sensible and latent heat storage unit integrated with solar water heating system, Journal of Solar Energy Engineering, Transactions of the ASME, 131 (2009) 0410021-0410028.
[15] Y. Varol, A. Koca, H.F. Oztop, E. Avci, Forecasting of thermal energy storage performance of Phase Change Material in a solar collector using soft computing techniques, Expert Systems with Applications, 37 (2010) 2724-2732.
[16] R. Padovan, M. Manzan, Genetic optimization of a PCM enhanced storage tank for Solar Domestic Hot Water Systems, Solar Energy, 103 (2014) 563-573.
[17] H.S. Xue, Experimental investigation of a domestic solar water heater with solar collector coupled phase-change energy storage, Renewable Energy, 86 (2016) 257-261.
[18] A. Papadimitratos, S. Sobhansarbandi, V. Pozdin, A. Zakhidov, F. Hassanipour, Evacuated tube solar collectors integrated with phase change materials, Solar Energy, 129 (2016) 10-19.
[19] M.S. Naghavi, O.K. Seng, I.A. Badruddin, M. Mehrali, M. Silakhori, H.S.C. Metselaar, Theoretical model of an evacuated tube heat pipe solar collector integrated with phase change material, Energy, (2015).
[20] J.A. Duffie, W.A. Beckman, Solar Engineering of Thermal Processes, Wiley, 2013.
[21] N. Zhu, K. Vafai, Analysis of cylindrical heat pipes incorporating the effects of liquid–vapor coupling and non-Darcian transport—a closed form solution, International Journal of Heat and Mass Transfer, 42 (1999) 3405-3418.
[22] V. Alexiades, A.D. Solomon, Mathematical Modeling of Melting and Freezing Processes, Taylor & Francis Group, 1993.

[23] P. Armstrong, D. Ager, I. Thompson, M. McCulloch, Domestic hot water storage: Balancing thermal and sanitary performance, Energy Policy, 68 (2014) 334-339.
[24] J. Fernandez-Seara, F.J. Uhía, J. Sieres, Experimental analysis of a domestic electric hot water storage tank. Part I: Static mode of operation, Applied thermal engineering, 27 (2007) 129-136.
[25] P. Armstrong, D. Ager, I. Thompson, M. McCulloch, Improving the energy storage capability of hot water tanks through wall material specification, Energy, 78 (2014) 128-140.
[26] B. Standard, In-situ formed dispensed rigid polyurethane and polisocyanurate foam products, in: British Standard BS EN 14318-1 2013, British Standards Institute, 2013.
[27] A. Faghri, Review and advances in heat pipe science and technology, Journal of Heat Transfer, 134 (2012).
[28] N. Ukrainczyk, S. Kurajica, J. Šipušić, Thermophysical comparison of five commercial paraffin waxes as latent heat storage materials, Chemical and Biochemical Engineering Quarterly, 24 (2010) 129-137.
[29] P. Lamberg, K. Siren, Analytical model for melting in a semi-infinite PCM storage with an internal fin, Heat and mass transfer, 39 (2003) 167-176.
[30] T.M.V.M. Association, Recommended Code of Practice for Safe Water Temperatures, in, BEAMA, London, England, 2013.

Nomenclature

Symbols

A_p	Pipe inner surface area	t_{CHE}	PCM thickness in CHE mode
$A_{c,c}$	Cross section area of the fin on HPC	t_{DHE}	PCM slab thickness in DHE mode
$A_{f,c}$	Face area of the fin on the HPC	$t_{f,CHE}$	Thickness of fin on heat pipe
$c_{p,l}$	Specific heat of liquid PCM	$t_{f,DHE}$	Thickness of fin on water pipe
$c_{p,s}$	Specific heat of solid PCM	t_{hp}	Thickness of the heat pipe wall
$c_{p,w}$	Specific heat of water	t_{wck}	Thickness of the wick
$d_{i,p}$	Pipe inner diameter	T_{amb}	Ambient temperature
d_w	Mesh wire diameter	T_{hp}	Heat pipe surface temperature
d_t	Glass tube outer diameter	T_m	PCM melting temperature
E_d	Total delivered energy	T_{pcm}	PCM temperature
g	Gravity	T_s	Cold water temperature
$h_{f,c}$	Fin height on the condenser	T_u	Water operating temperature
$h_{f,p}$	Fin height on pipe	$T_{w,b,i}$	Inlet water temperature in baseline system
h_{pcm}	Heat transfer coefficient in PCM	$T_{w,b,o}$	Outlet water temperature in baseline system
h_{st}	Storage tank height	$T_{w,i,i}$	Inlet water temperature in innovative system
h_w	Heat transfer coefficient in water	$T_{w,i,o}$	Outlet water temperature in innovative system
k_{eff}	Effective thermal conductivity of wick	$T_{w,t,i}$	Inlet water temperature to water storage tank
$k_{f,c}$	Thermal conductivity of fin on condenser	$T_{w,t,o}$	Outlet water temperature from water storage tank
$k_{f,p}$	Thermal conductivity of fin on pipe	V_u	Usable volume of hot water
k_l	Thermal conductivity of liquid PCM	$V_{u,\mathrm{d}}$	Destroyed usable volume of hot water
k_s	Thermal conductivity of solid PCM	$V_{u,\mathrm{r}}$	Remained usable volume of hot water
k_w	Thermal conductivity of heat pipe wall	w_{st}	Storage tank width
l_a	Length of heat pipe adiabatic region	X_{pcm}	Liquid-solid location in PCM slab
l_c	Length of heat pipe condenser region	Y_{pcm}	Solid-liquid location in PCM slab
l_e	Length of heat pipe evaporator region	**Greek**	
$l_{f,c}$	Fin length on the condenser	α_s	Thermal diffusivity [$= k_s/\rho_s c_s$]
$l_{f,p}$	Fin length on pipe	β_s	Slope of solar collector
l_p	Length of solar absorber plate	β_e	Expansion coefficient of the PCM
l_{st}	Storage tank length	ε	Porosity
$l_{st,s}$	Length of a section of the storage tank	θ	Angle of incidence
L	Latent heat of PCM	ρ_i	Diffuse reflectance of that surface
Lr	Usable volume loss rate percentage	ρ_g	Diffuse reflectance of the ground
$\dot{m}$	Water mass flow rate	ρ_l	Liquid PCM density
m_w	Mass of the stored hot water in water storage tank	ρ_s	Solid PCM density

N_a	Number of apertures per unit length of wick	ρ_w	Water density
N_f	Number of the fins	μ_{pcm}	Dynamic viscosity of the PCM
$P_{f,c}$	Perimeter of the fin on HPC	μ_w	Dynamic viscosity of the water
q	Heat flux	v_w	Mean velocity of water inside the pipe
S	Absorbed solar energy	ϕ	Latitude
St	Stefan number [$=c_l\Delta T_l/L$]	η	Efficiency